Site-Selective Deposition and Micropatterning of Visible-Light-Emitting Europium-Doped Yttrium Oxide Thin Film on Self-Assembled Monolayers

Yoshitake Masuda,[*,†,‡] Masao Yamagishi,[‡] and Kunihito Koumoto[‡]

National Institute of Advanced Industrial Science and Technology (AIST), 2266-98 Anagahora, Shimoshidami, Moriyama-ku, Nagoya 463-8560, Japan, and Graduate School of Engineering, Nagoya University, Nagoya 464-8603, Japan

We have developed a novel process for preparing a micropattern of europium-doped yttrium oxide thin films using a patterned self-assembled monolayer. The thin film was transformed into the crystalline phase by annealing at 800 °C for 1 h. Europium-doped yttrium oxide films showed red emission (611 nm) due to photoluminescence excited by 266 nm. The deposition and micropatterning of visible-light-emitting europium-doped yttrium oxide was successfully realized in an aqueous solution under environmentally friendly conditions.

Introduction

High-quality phosphors for excellent luminescence efficiency, color purity, sufficient brightness, and long-term stability are required to improve the performance of display devices. Extensive research has been carried out on rare-earth activated oxide phosphors due to their good luminescence characteristics, stability in high vacuum, and absence of corrosive gas emission under electron bombardment when compared to currently used sulfide-based phosphors to enhance the luminescence characteristics of phosphors.[1]

In particular, red-emitting europium-activated yttrium oxide (Y_2O_3:Eu) has attracted much attention both as one of the most promising oxide-based red phosphor systems[2,3] due to its excellent luminescence efficiency, color purity, and stability[4] and also as a model system for studying the effect of the interplay of radiative and nonradiative processes on phosphor efficiency. Y_2O_3:Eu exhibits strong UV and cathode-ray-excited luminescence with a quantum efficiency of nearly 100%[3] and is useful in lighting and cathode ray tubes, display materials, tricolor fluorescent lamps,[3,5,6] projection televisions,[3,7] field emission displays,[8,9] laser devices,

and so forth.[10−12] As an oxide, it is more stable than sulfur-containing phosphors which undergo changes in their surface chemistry when interacting with the electron beam, seriously degrading their cathodoluminescent brightness and releasing gases that can poison the field-emitting tips.

In the preparation of Y_2O_3:Eu nanoparticles, many different techniques have been reported such as solid-state reactions, spray pyrolysis,[12,13] chemical vapor deposition,[14] sol−gel reaction,[10,15] and so on. Phosphor particles (3−10 μm) without regular shape are prepared commercially by high-temperature solid-state reactions, resulting in large particles and agglomerates. Their size is reduced by mechanically grinding/milling, which leads to the formation of nonradiative defects and the introduction of nonradiative impurities, significantly reducing luminescence efficiency. The luminescence properties are highly dependent on crystalline size, crystallinity, Eu concentration, uniformity of Eu distribution, and so forth, which need to be improved and optimized in order to enhance the luminescence properties.

Here, we propose a novel process for synthesizing visible-light-emitting Y_2O_3:Eu using a solution system which has advantages in control of grain size, crystalline size and morphology, and high uniformity of Eu distribution. Phosphor particles can be prepared by our newly developed solution process without the formation of nonradiative defects and the introduction of nonradiative impurities caused by

* Corresponding author: e-mail, masuda-y@aist.go.jp.
† National Institute of Advanced Industrial Science and Technology (AIST).
‡ Nagoya University.

(1) Ropp, R. C. *The Chemistry of Artificial Lighting Devices: Lamps, Phosphors, and Cathode Ray Tubes*; Elsevier: New York, 1993.
(2) Jones, S. L.; Kumar, D.; Singh, R. K.; Holloway, P. H.; Singh, P. K. *Appl. Phys. Lett.* **1997**, *71*, 404−406.
(3) Blasse, G.; Grabmaier, B. C. *Luminescent Materials*; Springer: Berlin, 1994.
(4) Wakefield, G.; Holland, E.; Dobson, P. J.; Hutchison, T. L. *Adv. Mater.* **2001**, *13*, 1557−1560.
(5) Peters, T. E.; Pappalardo, R. G.; Hunt, R. B. J. In *Solid State Luminescence*; Katai, A. H., Ed.; Chapman & Hall: London, 1993; p 313.
(6) Ronda, C. R. *J. Lumin.* **1997**, *72−74*, 49−54.
(7) Blasse, G. In *Solid State Luminescence*; Katai, A. H., Ed.; Chapman & Hall: London, 1993; p 349.
(8) Holloway, P. H.; Trottier, T. A.; Abrams, B.; Kondoleon, C.; Jones, S. L.; Sebastian, J. S.; Thomes, W. J.; Swart, H. *J. Vac. Sci. Technol., B* **1999**, *17*, 758−764.

(9) Goldburt, E. T.; Bolchouchine, V. A.; Levonovitch, B. N.; Sochtine, N. P. *J. Vac. Sci. Technol., B* **1999**, *17*, 765−768.
(10) Rao, R. P. *J. Electrochem. Soc.* **1996**, *143*, 189−197.
(11) Qiang, S.; Barthou, C.; Denis, J. P. *J. Lumin.* **1983**, *28*, 1−11.
(12) Xu, C. Y.; Watkins, B. A.; Sievers, R. E.; Jing, X. P.; Trowga, P.; Gibbons, C. S.; Vecht, A. *Appl. Phys. Lett.* **1997**, *71*, 1643−1645.
(13) Kang, Y. C.; Roh, H. S.; Park, S. B. *J. Electrochem. Soc.* **2000**, *147*, 1601−1603.
(14) Sun, L. D.; Yao, J.; Liu, C.; Liao, C.; Yan, C. H. *J. Lumin.* **2000**, *87−89*, 447−450.
(15) Lee, M. H.; Oh, S. G.; Yi, S. C. *J. Colloid Interface Sci.* **2000**, *226*, 65−70.

Y_2O_3:Eu Thin Film Deposition and Micropatterning

Chem. Mater., Vol. 19, No. 5, 2007 **1003**

the grinding process. Additionally, a high degree of homogeneity is achievable in a solution, since all of the starting materials are mixed at the molecular level. Doping of Eu activator through solutions is straightforward, easy, and effective.[10]

In addition, we propose a novel process for preparing Y_2O_3:Eu particulate films on substrates directly from the solution without the pre-preparation of Y_2O_3:Eu powders to avoid damage to phosphors and degradation of luminescence properties during the particle size reduction process and the process of film formation from the powders.

Furthermore, microfabrication such as two-dimensional (2D) micropatterning of the Y_2O_3:Eu film is indispensable to fabricate display devices. Micropatterning of Y_2O_3:Eu films can be prepared by etching Y_2O_3:Eu; however, etching damage (i.e., the change of chemical composition, Eu concentration, Eu condition, crystallinity, grain size and crystallite size, the boundary separation between a phosphor film and a substrate, cracks in phosphor films, loss of the shape in the pattern, and damage to substrates) causes serious degradation of luminescence properties even though as-prepared Y_2O_3:Eu powder has high luminescence performance. Recently, site-selective deposition of oxide films was proposed and nano-/microfabrication such as 2D patterning of oxide films was realized utilizing self-assembled monolayers (SAMs).[16−21] Molecular recognition, chemical reaction, and various functions of organic head groups of SAMs were effectively used for controlling the nucleation, growth, and deposition of oxide materials based on scientific knowledge about the deposition mechanism[22] and interface phenomena. This scientific knowledge was acquired from precise investigation of the chemical reactions of ions and molecules, the mechanisms for heterogeneous nucleation, homogeneous nucleation, growth and deposition of oxide (both of thin films and particles), modification and functionality of head groups of SAMs, interaction between head groups of SAMs and ions (and molecules) such as molecular recognition, chemical reaction, zeta potential, and hydrophobic interaction, and the change of solution conditions with time such as concentration, pH, and temperature. Nano-/micropatterning of TiO_2 thin films having 200 nm line width, 100 nm interval, and 70 nm thickness was realized with site-selective deposition which is the finest pattern achieved in the solution,[23] and micropatterns of various oxides have been developed. We propose using the high performance of SAMs to achieve site-selective deposition of Y_2O_3:Eu to fabricate visible-light-emitting 2D micropatterns.
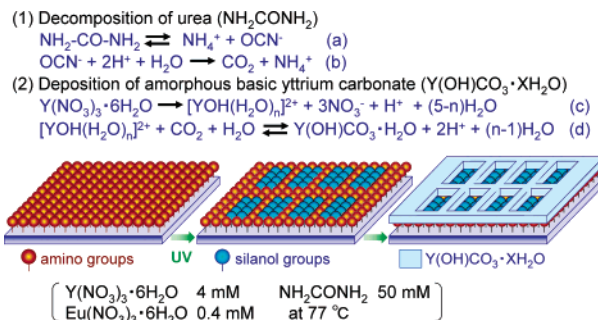
(16) Aizenberg, J.; Black, A. J.; Whitesides, G. M. *Nature* **1999**, *398*, 495−498.
(17) Aizenberg, J.; Black, A. J.; Whitesides, G. M. *J. Am. Ceram. Soc.* **1999**, *121*, 4500−4509.
(18) Masuda, Y.; Sugiyama, T.; Lin, H.; Seo, W. S.; Koumoto, K. *Thin Solid Films* **2001**, *382*, 153−157.
(19) Masuda, Y.; Jinbo, Y.; Yonezawa, T.; Koumoto, K. *Chem. Mater.* **2002**, *14*, 1236−1241.
(20) Masuda, Y.; Sugiyama, T.; Koumoto, K. *J. Mater. Chem.* **2002**, *12*, 2643−2647.
(21) Masuda, Y.; Ieda, S.; Koumoto, K. *Langmuir* **2003**, *19*, 4415−4419.
(22) Masuda, Y.; Sugiyama, T.; Seo, W. S.; Koumoto, K. *Chem. Mater.* **2003**, *15*, 2469−2476.
(23) Masuda, Y.; Saito, N.; Hoffmann, R.; De Guire, M. R.; Koumoto, K. *Sci. Technol. Adv. Mater.* **2003**, *4*, 461−467.

Figure 1. Conceptual process for site-selective deposition of visible-light emitting Y_2O_3:Eu thin films using a SAM.
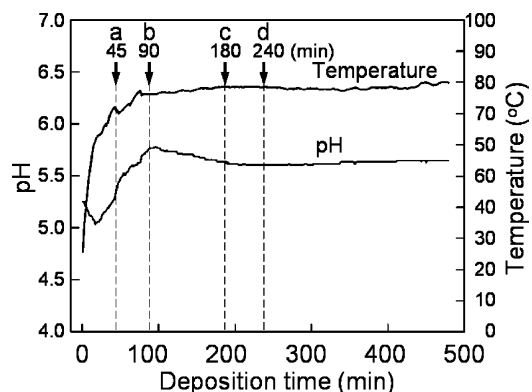

Figure 2. Time variation of pH and temperature of the solution.

Here, we propose and develop a novel process for achieving site-selective deposition of Y_2O_3:Eu and fabricate 2D micropatterns of visible-light-emitting Y_2O_3:Eu. The process allows us to avoid etching damage to the Y_2O_3:Eu and achieve precise control of grain size and crystalline size and high uniformity of Eu distribution. The scientific knowledge included in this site-selective deposition will contribute to the development of SCIS (solution chemistry for inorganic solids) which has been developed over several decades to fabricate novel functional inorganic materials. Control of nucleation, growth, and deposition of inorganic materials in the solution is the most basic and essential factor for solution chemistry for inorganic materials, and molecular recognition of functional head groups of SAMs will provide a novel scientific field for SCIS and controllability of the factors (nucleation, growth, and deposition of inorganic materials).

Experimental Section

SAM Preparation and Its Modification.[24−27] The Si substrate (p-type [100], 1−50 Ω cm, Newwingo Co., Ltd.) was cleaned ultrasonically in acetone, ethanol, and deionized water for 5 min, respectively, in this order and was exposed to ultraviolet light and ozone gas for 10 min to remove organic contamination by using a UV/ozone cleaner (184.9 and 253.7 nm; low-pressure mercury lamp 200 W, PL21-200, SEN Lights Co., 18 mW/cm², distance from lamp 30 mm, 24 °C, humidity 73%, air flow 0.52 m³/min, 100 V, 320 W). The APTS (3-aminopropyltriethoxysilane) SAM was prepared by immersing the Si substrate in an anhydrous toluene solution containing 1 vol % APTS for 1 h in a N_2 atmosphere. The substrate was rinsed with a fresh anhydrous toluene in a N_2 atmosphere. The substrate with the SAM was baked at 120 °C for 5 min to remove residual solvent and promote chemisorption of the SAM.

1004 *Chem. Mater., Vol. 19, No. 5, 2007*
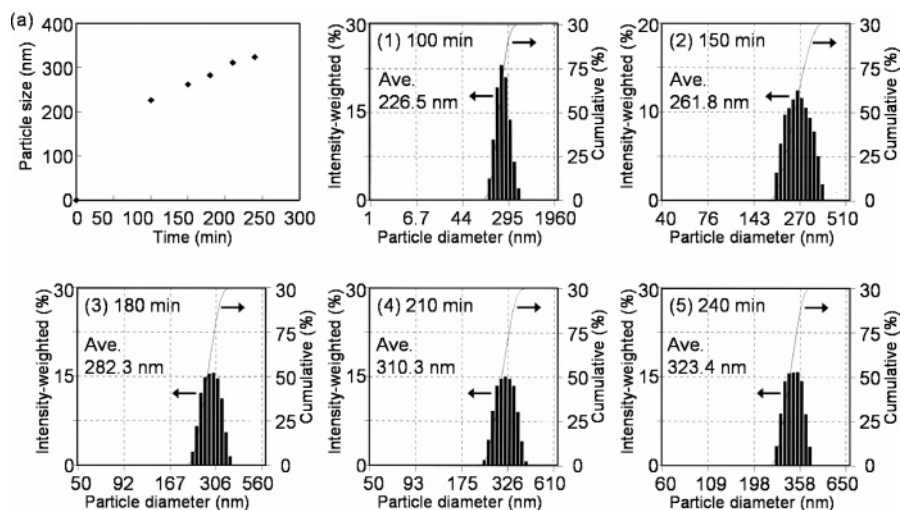
Masuda et al.

Figure 3. (a) Time variation of particle size distribution. (1−5) Particle size distribution of yttrium carbonate particles at (1) 100 min, (2) 150 min, (3) 180 min, (4) 210 min, or (5) 240 min.
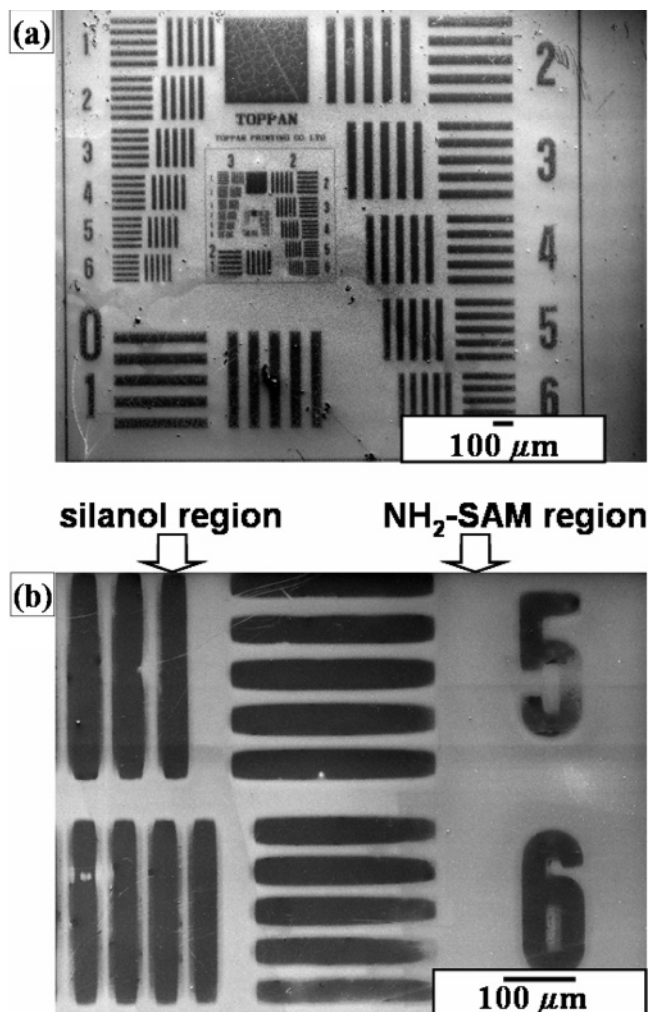

Figure 4. (a) SEM micrograph of patterned Y_2O_3:Eu thin films and (b) magnified area of part a.

APTS-SAM was then irradiated by ultraviolet light (PL21-200) through a photomask (test chart no. 1, N type, quartz substrate, 1.524 mm thickness, guaranteed line width 2 μm ± 0.5 μm, Toppan Printing Co., Ltd.) for 10 min. UV irradiation modified an amino-terminated silane to a silanol forming a pattern of amino-terminated silane regions and silanol regions.[24−27] Patterned APTS-SAM having amino regions and silanol regions was used as a template for patterning of yttrium oxide. Initially deposited APTS-SAM showed water contact angles (WCAs) of 48°. The UV-irradiated surface of the SAM was, however, wetted completely (contact angle <5°). This suggests that the SAM of APTS was modified to hydrophilic OH group surfaces by UV irradiation.

Characterization. The pH and temperature of the solution were measured and recorded by a pH meter (Cyberscan 1100, Eutech Instruments Pte, Ltd.) connected to a computer. The size distribution of homogeneously nucleated particles in the solution was measured by an electrophoretic light scattering instrument (ELS-8000, Otsuka Electronics Co., Ltd.). After having been immersed in the solution, the substrates were rinsed with distilled water and observed by a scanning electron microscope (SEM; S-3000N, Hitachi, Ltd.) and a scanning probe microscope (SPI 3800N, Seiko Instruments, Inc.) that was operated in AFM (atomic force microscopy) tap mode to observe the topography of the surface. AFM scans were performed at room temperature under ambient air. The ratio of Y:Eu was evaluated by energy dispersive X-ray analysis (EDX; EDAX Falcon, EDAX Co., Ltd.), which is built into the SEM. The surface of thin films was evaluated by X-ray photoelectron spectroscopy (XPS; ESCALAB 210, VG Scientific, Ltd.) in which the X-ray source (Mg Kα, 1253.6 eV) was operated at 15 kV and 18 mA and the analysis chamber pressure was $1-3 \times 10^{-7}$ Pa. Crystal phases of phase transition were evaluated by X-ray diffraction (XRD; RINT-2100, Rigaku) with Cu Kα radiation (40 kV, 30 mA) and a Ni filter plus a graphite monochromator. The crystal structure model and diffraction pattern of Y_2O_3 were calculated from ICSD (Inorganic Crystal Structure Database) data (FIZ Karlsruhe, Germany, and NIST, U.S.A.) using FindIt and ATOMS (Hulinks, Inc.). Photoluminescence images of the films were taken with a digital camera (Coolpix 8400, 8.0 megapixels, Nikon Corp.), and photoluminescence spectra were evaluated by a fluorescence spectrometer (F-4500, excitation wavelength 350 nm, Xe lamp, Hitachi, Ltd.).

Results and Discussion

Synthesis of Yttrium Oxide. The patterned APTS-SAM was immersed in an aqueous solution containing $Y(NO_3)_3 \cdot$

(24) Dressick, W. J.; Calvert, J. M. *Jpn. J. Appl. Phys.* **1993**, *32*, 5829−5839.
(25) Collins, R. J.; Shin, H.; De Guire, M. R.; Heuer, A. H.; Sukenik, C. N. *Appl. Phys. Lett.* **1996**, *69*, 860−862.
(26) Masuda, Y.; Koumura, T.; Okawa, T.; Koumoto, K. *J. Colloid Interface Sci.* **2003**, *263*, 190−195.
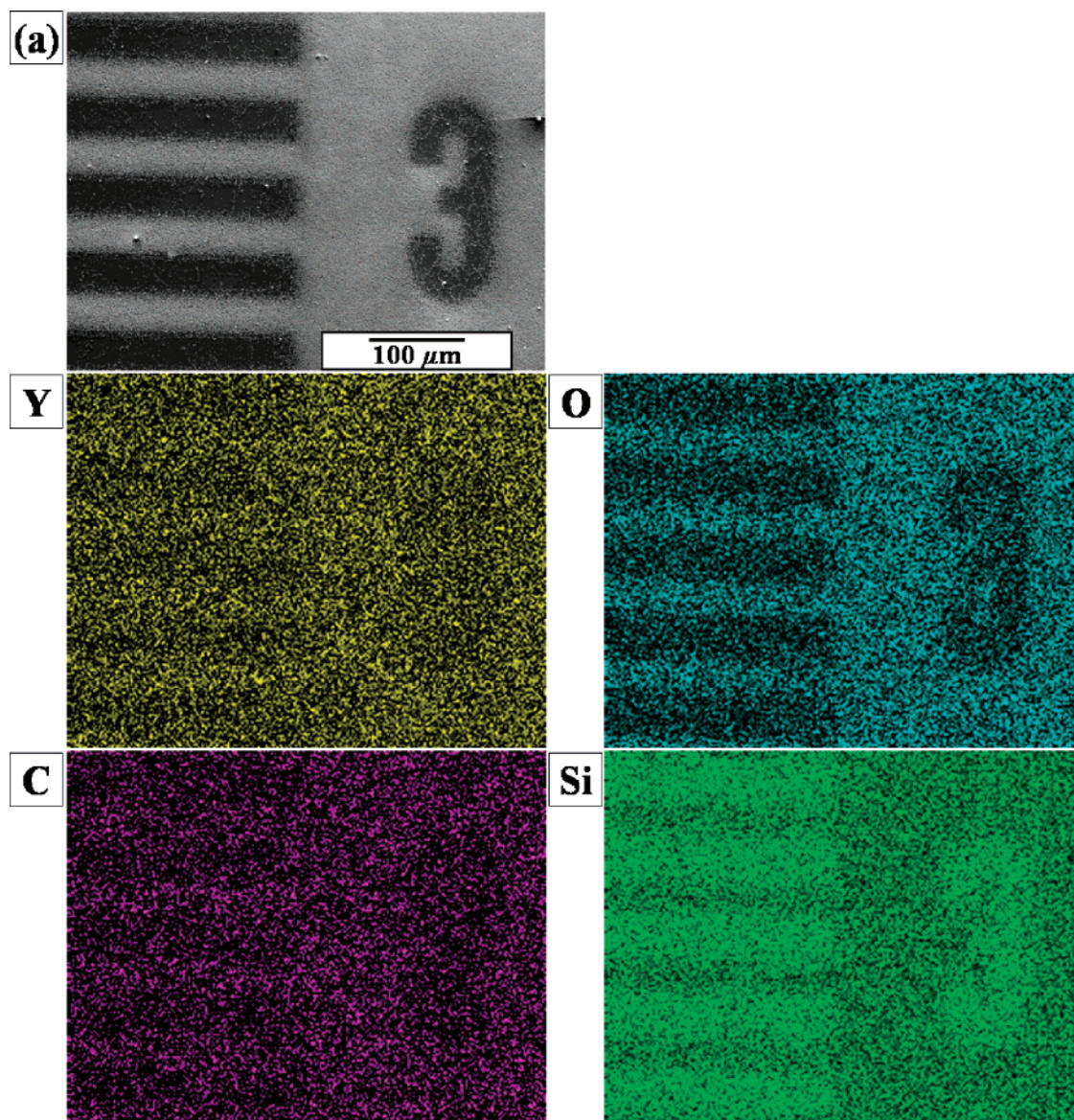(27) Masuda, Y.; Itoh, M.; Yonezawa, T.; Koumoto, K. *Langmuir* **2002**, *18*, 4155−4159.

Figure 5. (a) SEM micrograph of patterned Y_2O_3:Eu thin films. Characteristic X-ray images of Y, O, C, and Si for (a) Y_2O_3:Eu thin films.
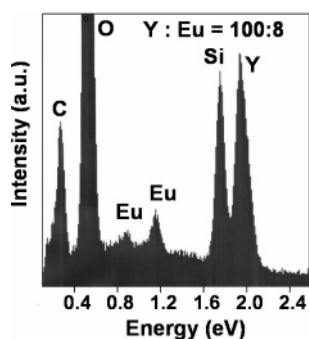

Figure 6. Elemental analysis of Y_2O_3:Eu thin films deposited for 90 min.

Cyanate ions react rapidly according to eq (b). Yttrium ions are weakly hydrolyzed[29,30] in water to $YOH(H_2O)_n^{2+}$ (eq (c)). The resulting release of protons (H^+) and/or hydronium ions (H_3O^+) accelerates urea decomposition (eq (b)). The precipitation of the amorphous basic yttrium carbonate ($Y(OH)CO_3 \cdot xH_2O$, $x = 1$) can take place through the reaction in eq (d).[31,32] The controlled release of cyanate ions by urea decomposition causes deposition of basic yttrium carbonate once the critical supersaturation in terms of reacting component is achieved. Since the decomposition of urea is quite slow, the amount needed to reach supersaturation within a given period of time must be considerably higher than the

$6H_2O$ (4 mM), $Eu(NO_3)_3 \cdot 6H_2O$ (0.4 mM), and NH_2CONH_2 (50 mM) at 25 °C. The solution was heated to 77 °C gradually as shown in Figure 1 since urea (NH_2CONH_2) decomposes to form ammonium ions (NH_4^+) above 70 °C (eq (a)). The decomposition of urea at elevated temperature plays an essential role in the deposition of yttrium oxide. The aqueous solution of urea yields ammonium ions and cyanate ions (OCN^-) at temperatures above 70 °C[28] (eq (a)).

(28) Shaw, W. H. R.; Bordeaux, J. J. *J. Am. Chem. Soc.* **1955**, *77*, 4729−4733.
(29) Ryabchikov, D. E.; Ryabukhin, V. A. *Analytical Chemistry of Yttrium and the Lanthanide Elements*; Humphrey Science: Ann Arbor, MI, 1970.
(30) Baes, C. F.; Mesmer, R. E. *The Hydrolysis of Captions*; Wiley: New York, 1976.
(31) Aiken, B.; Hsu, W. P.; Matijevic, E. *J. Am. Ceram. Soc.* **1988**, *71*, 845−853.
(32) Agarwal, M.; DeGuire, M. R.; Heuer, A. H. *Appl. Phys Lett.* **1997**, *71*, 891−893.
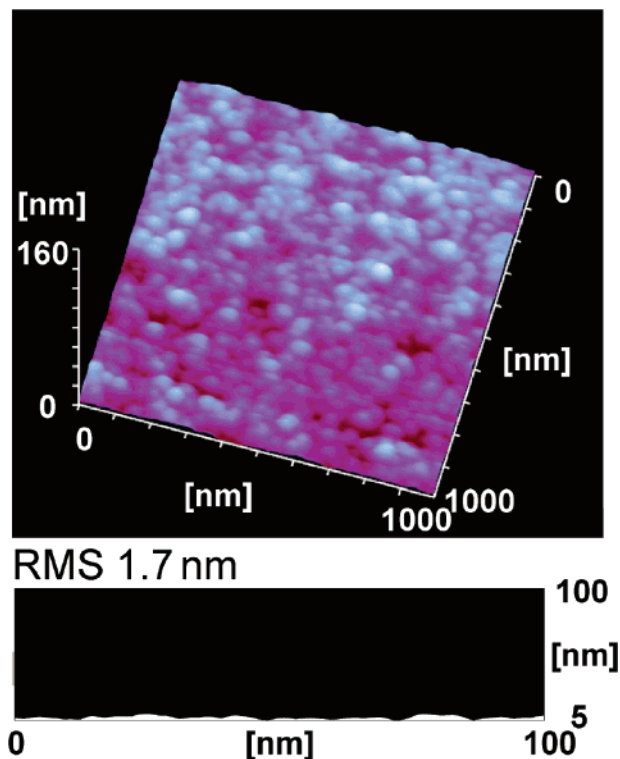
(a) NH₂ groups regions
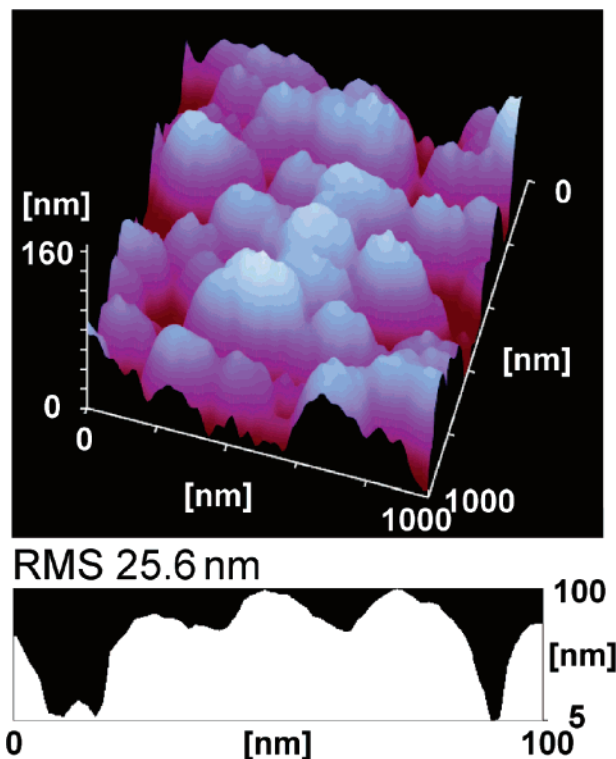
(b) OH groups regions

Figure 7. (a) AFM images and cross-section profile of Y_2O_3:Eu thin films on NH₂ groups regions. (b) AFM images and cross-section profile of Y_2O_3:Eu thin films on OH groups regions.

stoichiometric amount of yttrium ions, as revealed by previous studies of lanthanide compounds.[33]

The temperature of the solution increased gradually and reached 77 °C in about 80 min as shown in Figure 2. The solution was kept at ∼77 °C during deposition. The pH of the solution increased from 5.2 to 5.8 in about 90 min and then gradually decreased to 5.6. Temperature and pH increased for the initial 90 min and became stable after 90 min. The average size of particles homogeneously nucleated in the solution at 100 min was about 227 nm and increased to 262 nm at 150 min, 282 nm at 180 min, 310 nm at 210 min, and 323 nm at 240 min (Figure 3). Particles nucleated and grew after the solution temperature exceeded 70 °C because urea decomposes above 70 °C to form carbonate ions[28] which causes deposition of basic yttrium carbonate.[29−32] The particles grew rapidly at the beginning of the growth period, and then their growth rate decreased exponentially (Figure 3). The decrease in growth rate was caused by the decrease of supersaturation degree influenced by a decrease in solution concentration.

Patterning of Yttrium Oxide. Yttrium carbonate films were observed to deposit on amino regions of a patterned SAM after the immersion in an aqueous solution (Figure 4). Deposits showed white contrast, while silanol regions without deposition showed black contrast in SEM observation. Narrow lines of depositions having 10−50 μm width were successfully fabricated in an aqueous solution. Patterned APTS-SAM showed high ability for site-selective deposition of yttrium carbonate in solution systems.

Yttrium carbonate films were also deposited on the hydrophobic octadecyl surface of OTS (octadecyltrichlorosilane)-SAM having WCA of 116° and as-purchased silicon wafer having WCA of about 20−50° which was kept in a plastic case in air. On the other hand, the films were not deposited on UV irradiated silicon wafer having WCA < 5°. The super hydrophilic surface of WCA < 5° suppressed film deposition, whereas the hydrophobic surface and medium surface of WCA > 20−30° accelerated film deposition possibly because of hydrophobic interaction between deposition and substrate surface. This is consistent with a former study.[32] Yttrium carbonate was deposited both on bare single-crystal Si wafers and on Si wafers coated with sulfonate-functionalized organic SAMs.

Yttrium, europium, oxygen, and carbon were observed from as-deposited thin films on amino regions, while silicon and oxygen were detected from non-covered silanol regions by EDX (Figure 5). The molecular ratio of yttrium to europium was determined to be 100:8 (Figure 6). It was close to that of $Y(NO_3)_3 \cdot 6H_2O$ to $Eu(NO_3)_3 \cdot 6H_2O$, that is, 100:10, in the solution because the chemistry of $Eu(NO_3)_3$ is similar to that of $Y(NO_3)_3$ to incorporate europium in the precipitation. The content of europium was in the range we had expected. Y_2O_3:Eu with atomic ratio Y/Eu = 100:∼8 was reported to have strong photoluminescence.[34,35] Carbon was detected from yttrium carbonate. Silicon and oxygen were detected from a silicon wafer covered with a natural oxide layer (amorphous SiO_2).

(33) Matijevic, E.; Hsu, W. P. *J. Colloid Interface Sci.* **1987**, *118*, 506−523.

(34) Sharma, P. K.; Jilavi, M. H.; Nass, R.; Schmidt, H. *J. Lumin.* **1999**, *82*, 187−193.

(35) Kwaka, M. G.; Parkb, J. H.; Shon, S. H. *Solid State Commun.* **2004**, *130*, 199−201.
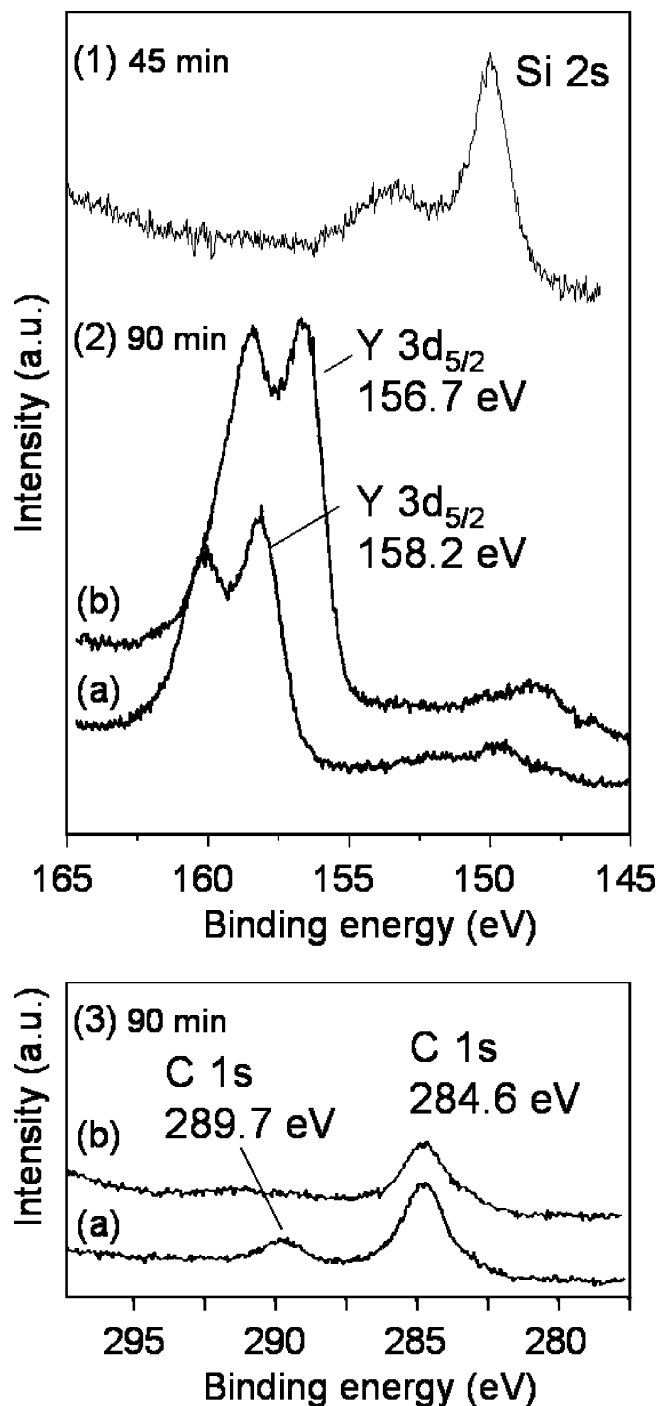
Figure 8. (1) XPS spectrum of Y 3d and Si 2s for Y_2O_3:Eu thin films deposited for 45 min. (2) XPS spectra of Y 3d and Si 2s for Y_2O_3:Eu thin films deposited for 90 min (a) before and (b) after annealing at 800 °C for 1 h. (3) XPS spectra of C 1s for Y_2O_3:Eu thin films deposited for 90 min (a) before and (b) after annealing at 800 °C for 1 h.

Figure 9. XRD patterns of Y_2O_3:Eu thin films (a) before and (b) after annealing at 800 °C for 1 h. (The upper picture) Crystal structure model and diffraction pattern of cubic Y_2O_3 calculated from crystal structure data of ICSD #23811.

Amino regions were covered with thin films composed of many large particles (about 100−300 nm in diameter) and very high roughness (root mean square, rms, 25.6 nm; Figure 7). Silanol regions, on the other hand, showed only nanosized small particles (about 10−50 nm in diameter) and very low roughness (rms 1.7 nm). The high site selectivity of deposition and the big difference in surface morphology and roughness were clearly shown by AFM observation. The thickness of the films was estimated from AFM scans across deposited and undeposited regions of the substrate. It increased with immersion time after 45 min (0 nm at 45 min,
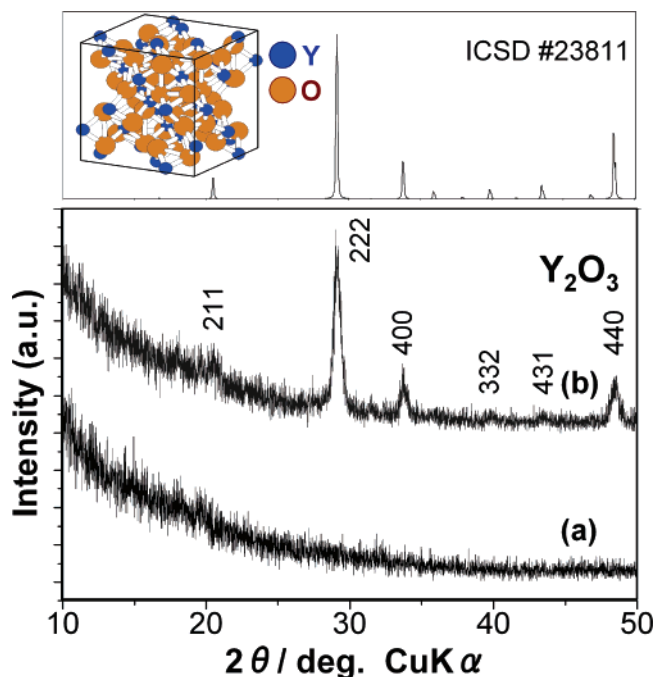
60 nm at 70 min, and 100 nm at 90 min (Figure 7)). The average growth rate (70 nm/h = 100/90 min) was higher than that previously reported (2 nm/h = 35 nm/15 h).[32] An amorphous yttrium basic carbonate film was deposited at 80 °C from aqueous solutions of $YNO_3 \cdot 5H_2O$ and urea on Si wafers coated with sulfonate-functionalized organic SAMs in previous studies. The thickness was then evaluated by transmission electron microscopy after the treatment with ultrasonication for 1/2 h in distilled water. The difference of growth rate was caused mainly by the difference of the substrate treatment by ultrasonication. Additionally, the thickness of our film was smaller than the particle size in the solution shown in Figure 3 (227 nm at 100 min). Heterogeneous nucleation and attachment of initial particles of yttrium carbonate occurred without the attachment of aggregated large particles shown in Figure 3. The yttrium carbonate was then grown on the substrate to form a film of 100 nm thickness after immersion for 90 min. The particles of about 100 nm in height were removed by ultrasonication for 30 min, and the film of several nanometers in height remained as reported.[32]

Yttrium was not detected by the XPS from the substrate immersed for 45 min (Figure 8-1); however, it was clearly observed from that immersed for 90 min (Figure 8-2a). This indicates that the deposition began between 45 and 90 min after immersion. The solution temperature reached 70 °C in ∼ 45 min (Figure 2) and then the solution began to decompose and release carbonate ions, causing the deposition of basic yttrium carbonate. The deposition mechanism evaluated by XPS is consistent with the change of solution temperature, decomposition temperature of urea, and chemical reaction of this system. The binding energy of the Y $3d_{5/2}$ spectrum from the deposition (158.2 eV; Figure 8-2a) was higher than that of metal yttrium (155.8 eV).[36] The spectrum
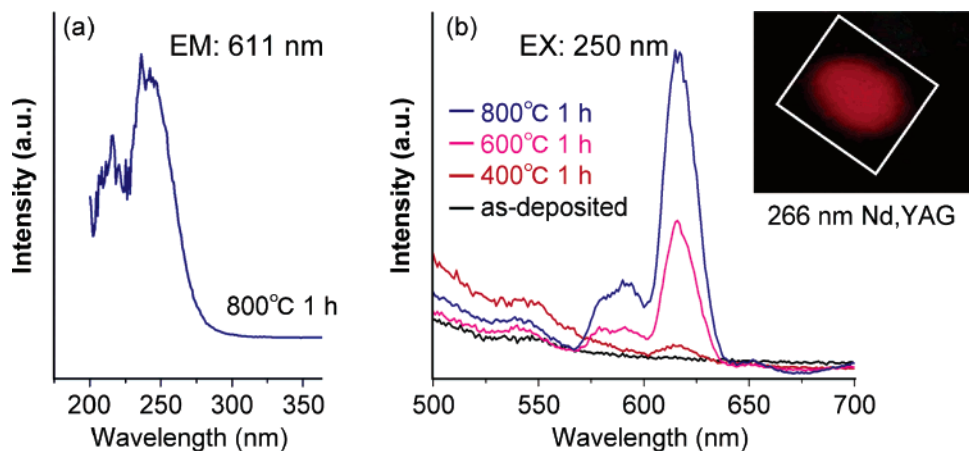
Figure 10. (a) Fluorescence excitation spectrum (emission: 611 nm) for Y_2O_3:Eu thin film after annealing at 800 °C for 1 h. (b) Fluorescence emission spectra (excitation: 250 nm) for Y_2O_3:Eu thin films before and after annealing at 400, 600, or 800 °C for 1 h. Inset: Photoluminescence image for Y_2O_3:Eu thin film annealed at 800 °C for 1 h (excitation: 266 nm).

shifted to lower binding energy (156.7 eV) after annealing at 800 °C in air for 1 h (Figure 8-2b) and is similar to that of Y_2O_3 (157.0 eV).[37] The binding energies of Y $3d_{5/2}$ spectra in as-deposited films and annealed films were higher than that of metal yttrium possibly because of the chemical bonds formed between yttrium ions and oxygen ions. The chemical shift of the Y $3d_{5/2}$ binding energy by annealing is consistent with crystallization of as-deposited films to crystalline Y_2O_3. C 1s spectra were detected at 289.7 and 284.6 eV from as-deposited films (Figure 8-3a). The C 1s spectrum at 289.7 eV then disappeared by the annealing (Figure 8-3b). C 1s at 284.6 eV was assigned to surface contamination, and C 1s at 289.7 eV was detected from as-deposited yttrium carbonate. The disappearance of C 1s at 289.7 eV is consistent with the phase transition from yttrium carbonate to Y_2O_3.

As-deposited film was shown to be an amorphous phase (Figure 9a) by XRD measurement. The film showed no diffraction peak after annealing at 400 °C for 1 h; however, it showed 222, 400, and 440 diffraction peaks of crystalline cubic Y_2O_3[38] without any additional phase after annealing at 600 °C for 1 h, and the intensities of diffraction peaks increased further by annealing at 800 °C for 1 h (Figure 9b). The film was shown to be a polycrystalline Y_2O_3 film constructed from randomly deposited Y_2O_3 particles without crystal-axis orientation. The crystal structure model and diffraction pattern of Y_2O_3 were calculated from the crystal structure data of ICSD #23811 as shown in Figure 9. The crystallization by annealing confirmed from XRD measurement is consistent with XPS evaluation.

We attempted to remove Y_2O_3 films from the silicon substrate by debonding with scotch tape or by ultrasonication for 5 min in water. However, the films maintained their bonds with the substrate, indicating that strong adhesion had formed between films and substrate.

The thin film annealed at 800 °C for 1 h, that is, crystalline Y_2O_3:Eu thin film, was shown to be excited by 230–250 nm (center: 243 nm) and emit red light photoluminescence centered at 611 nm in the fluorescence excitation spectrum (Figure 10a). Neither the as-deposited film nor the film annealed at 400 °C for 1 h showed photoluminescence; on the other hand, the films annealed at 600 °C or 800 °C for 1 h emitted light centered at 617 nm by 250 nm in fluorescence emission spectra (Figure 10b). The fluorescence intensity of the film annealed at 800 °C was stronger than that of the film annealed at 600 °C. Fluorescence intensity increased by the phase transformation from amorphous yttrium carbonate to yttrium oxide and crystal growth by the heat treatments and is consistent with the crystallization observed by XRD.[32] The spectra are described by the well-known $^5D_0$–^7F_J line emissions ($J = 0, 1, 2, ...$) of the Eu^{3+} ion with the strongest emission for $J = 2$ at 612 nm. The thin film annealed at 800 °C produced visible red light photoluminescence by excitation from the Nd:YAG laser (266 nm; Figure 10, inset). The white square shows the edges of the Y_2O_3:Eu thin film, and the red color shows visible red emission from the irradiated area on the substrate.

Conclusions

In summary, we have proposed a novel process for fabricating visible red light emitting Eu-doped Y_2O_3 and its micropattern using a SAM and an aqueous solution system. The patterned APTS-SAM having amino group regions and silanol group regions achieved site-selective deposition of yttrium oxide in an aqueous solution. The deposited films were crystallized by annealing at 600 °C or 800 °C for 1 h. Crystalline Y_2O_3:Eu produced visible red light photoluminescence centered at 611 nm by excitation from Nd:YAG laser (266 nm). This study showed the high potential of aqueous solution systems and SAMs for the fabrication of functional metal oxide thin films and their micropatterns.

(36) Fuggle, J. C.; Martensson, N. *J. Electron Spectrosc. Relat. Phenom.* **1980**, *21*, 275.
(37) Wagner, C. D. *Practical Surface Analysis*, 2nd ed.; John Wiley: New York, 1990; Vol. 1.
(38) Paton, M. G.; Maslen, E. N. *Acta Crystallogr.* **1967**, *1*, 1948–1923.